

REMARKS

REVIEW

The original application set forth claims 1-16 of which each of claims 1-7 and 13 were independent claims. The current application (as presently amended) sets forth claims 1-16 of which claims 1-7 and 13 are independent claims. Presently, no claims have been indicated as allowed in view of the prior art. Claims 9, 10, 15, and 16 stand objected to as being dependent on a rejected base claim, but are indicated as allowable if rewritten in independent form including all the limitations of the base claim and any intervening claims. Additionally, the specification is objected to for various informalities. Further, the drawings stand objected to as failing to comply with 37 CFR 1.84(p)(4) and 1.84(p)(5) because they include reference numbers not included in the specification and use one reference number to indicate two different elements.

Further still, claims 1, 2, 5, 7, 8, and 11 stand collectively rejected under 35 U.S.C. § 102(b) as being anticipated by Yamada et al. (U.S. Patent No. 5,517,017). Finally, claims 3, 4, 6, and 12-14 stand collectively rejected under 35 U.S.C. § 103(a) as unpatentable over Yamada et al.

DRAWING OBJECTIONS

Replacement drawings including correction of the various 37 CFR 1.84(p)(4) and 1.84(p)(5) errors is included herewith. As required a marked-up redline version of the corrections is included along with a clean version of the replacement figures for approval by the Examiner. It should be noted that Figure 11 is hereby withdrawn.

SPECIFICATION OBJECTIONS

It is respectfully submitted that the present objection to the specification is moot in view of the substitute specification submitted herewith. As mentioned above, both a marked-up copy of the substitute specification in compliance with the revised format for making amendments as set forth in 37 C.F.R. § 1.121 and a clean version of the substitute specification are attached hereto for the Examiner's approval.

35 U.S.C. §102(b) REJECTION

With respect to the 35 U.S.C. §102(b) rejection of claims 1, 2, 5, 7, 8, and 11, and in view of the significant distinctions discussed herein, Applicants respectfully traverse such ground of rejection with the above amendments and the following remarks.

As discussed in greater detail below, independent claims 1-7 and 13 encompass certain common aspects that distinguish them from the proposed reference. It is respectfully submitted that the reference, Yamada et al., merely serves to demonstrate the patentability of Applicant's claimed invention. Specifically, Yamada fails to adequately disclose every element of the claimed invention and as such cannot serve at law as an anticipating reference to the present invention under 35 U.S.C. §102.

Before setting forth a discussion of the prior art applied in the Office Action, it is respectfully submitted that controlling case law has frequently addressed rejections under 35 U.S.C. §102.

"For a prior art reference to anticipate in terms of 35 U.S.C. Section 102, **every element** of the claimed invention **must** be **identically** shown in a single reference." Diversitech Corp. v. Century Steps, Inc., 850 F.2d 675, 677, 7 U.S.P.Q.2d 1315, 1317 (Fed. Cir. 1988; emphasis added). The disclosed elements must be arranged as in the claim under

review. See Lindemann Machinefabrik v. American Hoist & Derrick Co., 730 F.2d 1452, 1458, 221 U.S.P.Q. 481, 485 (Fed. Cir. 1984). If any claim, element, or step is absent from the reference that is being relied upon, there is no anticipation. Kloster Speedsteel AB v. Crucible, Inc., 793 F.2d 1565, 230 U.S.P.Q. 81 (Fed. Cir. 1986; emphasis added). In PTO proceedings, claim language should be read in light of the specification as it would be interpreted by one of ordinary skill in the art. In re Sneed, 710 F.2d 1544, 1548, 218 U.S.P.Q. 385, 388 (Fed. Cir. 1983). The following analysis of the present rejections is respectfully offered with guidance from the foregoing controlling case law decisions.

Specifically, independent claims 1-7 and 13 each require a monolithic silicon integrated circuit not the hybrid thin film integrated circuit of Yamada et al. As specified in the abstract and elsewhere, the photosensor of Yamada et al. is formed by sequential deposition of thin films onto a substrate. A monolithic integrated circuit is one in which the elements of the circuit are formed within or in place on a semiconductor substrate.

Based upon this significant distinction and the above amendments, it is respectfully submitted that the use of Yamada et al. to anticipate any of claims 1, 2, 5, 7, 8, and 11 is improper. Acknowledgement of the same and withdrawal of the current grounds of rejection is earnestly solicited.

35 U.S.C. §103(a) REJECTIONS

In view of the above amendments and the significant distinctions discussed above, Applicant respectfully traverses such grounds of rejection. By relying on rejection grounds under 35 U.S.C. §103(a) for alleged obviousness, and by various statements throughout the detailed Office Action, the PTO already acknowledges certain important deficiencies of the

base reference Yamada et al. which renders such reference inadequate for serving by itself as a rejection basis for any of claims 3, 4, 6, and 12-14.

As discussed above Yamada et al. discloses a hybrid thin film integrated circuit. The present invention comprises a monolithic silicon integrated circuit on a chip for use in detecting the location and direction of a radiation source. As it is not known nor would it have been obvious in light of the known prior art to practice such source detection on a single monolithic silicon IC chip manufactured using planar silicon technology, it is respectfully submitted that the use of Yamada et al. as a basis for the 35 U.S.C. §103(a) rejection of claims 3, 4, 6, and 12-14 is improper. Withdrawal of such grounds of rejection is earnestly solicited.

CITED RELEVANT PRIOR ART

It is not believed that any of the prior art cited but not relied upon, alone or in combination either with each other or other cited prior art teaches, discloses, suggests or makes obvious the claimed features of the present invention.

CONCLUSION

In view of the foregoing amendments and comments, Applicants respectfully request withdrawal of the current grounds of objection and rejection and the issuance of a formal Notice of Allowance. The Examiner is invited to telephone the undersigned at his convenience should only minor issues remain after consideration of this amendment in order to permit early resolution of the same.

Respectfully submitted,
Lanier Ford Shaver & Payne, P.C.

8/26/04
Date

Charles R Ducker Jr
Charles R. Ducker, Jr.
Reg. No. 46,542
P.O. Box 2087
Huntsville, Alabama 35804-2087
Tel: 256.535.1100
Fax: 256.533.9322

LANIER FORD SHAVER & PAYNE P.C.
Customer Number 021491
P.O. Box 2087
Huntsville, Alabama 35804-2087
Phone: (256) 535-1100
Fax: (256) 533-9322

Certificate of Mailing under 37 C.F.R. § 1.8

I hereby certify that this correspondence is being deposited with the United States Postal Service with sufficient postage as first-class mail in an envelope address to: Mail Stop Non-Fee Amendment, Commissioner for Patents, P.O. Box 1450, Alexandria, VA 22313-1450, on **August 26, 2004**.

Charles R Ducker Jr
Signature

Charles R. Ducker, Jr.
Printed Name of Person Signing Certificate

MARKED-UP
COPY
OF
ORIGINAL
SPECIFICATION
AND
DRAWINGS

RADIATION SENSING INTEGRATED CIRCUIT DEVICE AND METHOD

CROSS-REFERENCE TO RELATED APPLICATIONS

This application claims the benefit of U.S. Provisional Application No. 60/224625, filed August 11, 2000, and entitled "RADIATION SENSING INTEGRATED CIRCUIT DEVICE AND METHOD". This provisional application is incorporated herein by reference.

BACKGROUND OF THE INVENTION

1. Field of the Invention

The present invention relates generally to the field of sensing devices, their use and methods for their manufacture, and more particularly, to a radiation sensing monolithic silicon integrated circuit for positional purposes. The device and method is particularly well suited integration in a monolithic silicon IC chip for use in navigation, guidance and control systems, for example systems in space or used for space exploration, or other systems including positional control of systems relative to incoming radiation.

2. Technical Background

Light (radiation) inherently contains direction and amplitude characteristics. Consequently, light (radiation) is useful in navigational and positional control applications. For example, sensors have been developed for use in vehicle guidance and control systems allowing navigation of vehicles relative to a light (radiation) source.

Positioning sensors that function in response to incident radiation are known in the art. One example of a guidance or a positioning system that uses a light or radiation source such as the sun for positioning is known in the art as a sun pointer. One such existing sun pointer system employs electro-optical sensing devices in conjunction with some type of mechanical alignment to guide the impinging light or radiation relative to the electro-optical sensors. **FIG. 1** illustrates a sun pointer system **100** that employs such

a design. The sensing element of system 100 is a photodiode array 106. Light (radiation) 108 impinges the array 106 through a mechanical entrance slit 104, providing direction and amplitude information to the system via photocell output signals 110, amplifiers 112, and buffer storage 114. Typical pointing systems of this type weigh approximately a quarter of a pound and require an input power of .25 to 1.0 watt.

U.S. Patent No. 4,611,914, entitled Sunbeam Incident Angle Detecting Device, illustrates a sun pointer system for determining position relative to a light source. The technology disclosed in the '914 patent uses a pair of solar cells disposed perpendicular to each other. When radiation impinges, the current produced by the radiation in the solar cells is used to determine the incident angle of the radiation. This angle is then used to determine the relative position of a satellite to a light source.

The existing technology for determining the position using the angle of incidence of radiation has several disadvantages. Some The optical systems currently in use are large, heavy, and require a significant amount of space to perform the sensing function required by the pointing system. In addition, some sun pointers in the prior art require significant power.

What is needed, but currently unavailable in the art, is an improved radiation sensing device that is small in size, capable of accurately providing information relating to directional position, light weight, and which has minimal power requirements for its use and operation. Such a device should be simple to use, easily adapted for use with existing equipment, and inexpensive to manufacture.

It is to the provision of such a device capable of providing azimuth and elevation information relative to incident radiation to the surface of a monolithic silicon IC chip that includes integral signal amplification that the present invention is primarily directed.

SUMMARY OF THE INVENTION

One aspect of the present invention is a system and method for determining the azimuth and elevation of radiation impinging the surface of ~~an~~ a monolithic silicon Integrated Circuit ("IC"). In order to determine azimuth and elevation of impinging radiation, a sensor detects the angle of incidence of impinging light (radiation) in both an x-plane and a y-plane relative to the chip surface. These rectangular coordinate outputs of the sensors can then be translated into spherical coordinates electronically as required. The angle of incidence information for the two planes provides the complete azimuth and elevation information.

Another aspect of the present invention is a monolithic silicon based directionally sensitive radiation sensor differential pair ("VCELL") fabricated using essentially conventional monolithic silicon integrated circuit ("IC") technologies. The sensor of the present invention is constructed on a standard silicon wafer. Differential pairs are formed ~~on~~ in the surface of the integrated circuit chip such that the angle of incidence of impinging radiation can be detected in both an x-plane and a y-plane. The differential pair consists of two NPN phototransistors formed in the <100> plane each having a P type base region or base extension formed in the <111> plane of the silicon. The <100> and <111> P type base regions are formed in a converging manner at a 54.7° angle. Such transistors provide amplification of the detected signals thus improving the noise performance of the device and results in an increased sensitivity to low level radiation signals.

Yet another aspect of the present invention relates to a system that determines the azimuth and elevation of radiation that is impinging the IC device of the present invention. The system includes the IC device described, *infra*, that detects the angle of incident of the impinging radiation in both an x-plane and a y-plane. The system further includes a circuit that performs calculations on the angle of incidence information detected by the integrated circuit to determine the azimuth and elevation of the impinging radiation.

Another aspect of the present invention is an IC as described, infra, having two VCELL structures and a reference monolithic silicon transistor. The reference transistor is a phototransistor formed in the <100> plane of the silicon chip. The reference transistor detects and amplifies impinging radiation to provide a normalization amplitude (or reference) value. Therefore, when calculating the angle of incidence of the radiation, the signals from each transistor of a single differential pair (VCELL) are subtracted. The difference (the differential output of a single VCELL structure) is may be divided (normalized) by the output of the reference transistor thus removing radiation amplitude from the final signal outputs of the sensor when computing azimuth and elevation.

The device, system, and method of the present invention allow for the miniaturization of radiation sensing. The miniaturized sensor of the present invention allows for the accurate determination of direction and position of an object relative to a known source of radiation. Further, the present invention provides a small, lightweight, rugged, low power and inexpensive device to be employed in vehicles or systems where size, weight and power are a factor such as vehicles for space applications. In addition, the miniature sensor may be used to detect increased solar radiation to reconfigure shielding on spacecraft during solar flares and storms. The sensor may also be used to prevent the inadvertent pointing of sensitive optical systems, such as in telescopes, at bright sources of radiation that might cause damage to sensitive detectors within some telescopes.

BRIEF DESCRIPTION OF THE DRAWINGS

The accompanying drawings, which are incorporated in and form a part of the specification, illustrate embodiments of the invention, and, together with the description, serve to explain the principles of the invention:

FIG. 1 (prior art) is a device employing a mechanical slit and electro-optical sensors in order to obtain the angle of incidence of impinging radiation.

FIG. 2 is a block diagram describing the functionality of the sensor monolithic silicon integrated circuit of the present invention and further including its relationship to a computational device or circuit contained within the same monolithic silicon chip.

5 **FIG. 3** is a cross-sectional view of ~~the typical~~ an exemplary VCELL structure of the present invention illustrating two <100> bipolar junction monolithic silicon phototransistors with opposing <111> base extensions (offset from each other by opposing <111> planes or an angle of 70.6 degrees).

10 **FIG. 4** is a circuit diagram modeling the VCELL structure of one exemplary embodiment of the present invention.

FIG. 5 is a circuit diagram modeling the dual-axes VCELL structure of one exemplary embodiment of the present invention.

15 **FIG. 6A & 6B** are graphs indicating the first order current behavior of the phototransistors of the IC.

20 **FIG. 7** is a photolithographic mask pattern diagram of an exemplary monolithic silicon IC of the present invention illustrating three VCELL structures, a reference transistor, some additional test structures, interconnect metallization and bond pads.

FIG. 8 is a diagram illustrating a topological view of a VCELL structure of the present invention (not drawn to scale).

25 **FIGS. 9A-9D** are successive topological views of the VCELL structure through the masking process steps during formation.

30 **FIGS. 10A-10H** illustrate cross-sectional views taken along line A-A in **FIG. 9**, of successive process steps for making an exemplary VCELL of the present invention.

FIG. 10I is a cross-sectional view, taken along line A'-A' in FIG. 9A.

~~FIG. 11 is a block diagram illustrating a system of the present invention having two separate and independent detector structures, the outputs of which are used to calculate azimuth and elevation of impinging radiation.~~

DETAILED DESCRIPTION OF THE PREFERRED EMBODIMENTS

Reference will now be made in detail to the present preferred embodiments of the invention, examples of which are illustrated in the accompanying drawings. Wherever possible, the same reference numerals will be used throughout the drawing figures to refer to the same or like parts. An exemplary embodiment of the present invention is a monolithic silicon based integrated circuit ("IC") capable of detecting light (radiation). An exemplary embodiment of the integrated circuit that detects radiation is described functionally in the block diagram in FIG. 2, and is designated generally throughout as reference numeral 116.

The monolithic silicon IC 116 includes an x-axis detector 118 capable of detecting the angle of incidence in an x-plane of impinging radiation, a y-axis detector 120 capable of detecting the angle of incidence in a y-plane, and a reference detector 122. The x-axis and the y-axis detectors, 118 and 120, have dual outputs that are amplified photocurrents caused in the detectors by the impinging radiation. The x-axis detector 118 has output currents I_{x1} and I_{x2} . The y-axis detector 120 has output currents I_{y1} and I_{y2} . The reference detector is a monolithic silicon phototransistor formed in the <100> plane of the silicon. The reference detector 122 is designed to provide a normalization current, I_{ref} , to factor out the amplitude of radiation impinging the surface of the IC. The net amplified generation recombination photocurrent ~~produced~~ computed in the x-axis detector 118 signal processing circuit 124 is I_x where

$$I_x = I_{x1} - I_{x2}$$

Therefore, I_x is the differential output of the x-axis detector 118. The normalized photocurrent output of the x-axis detector 118 is given by dividing the above by I_{ref} giving

5
$$I_x / I_{ref} = [I_{X1} - I_{X2}] / I_{ref}$$

The photocurrents produced in the y-axis detector are denoted as I_{y1} and I_{y2} . The net generation recombination photocurrent ~~produced~~ computed in the ~~y-axis detector~~ signal processing circuit 124 is I_y where

10
$$I_y = I_{Y1} - I_{Y2}.$$

Therefore, I_y is the differential output of the y-axis detector 120. Dividing by I_{ref} , the same as in 118, normalizes the outputs.

15 A preferred embodiment of the IC 116 can include two directionally sensitive radiation sensors or differential pairs ("VCELL") that are disclosed, supra. A VCELL device is used in the IC 116 as the x-axis detector 118 (FIG. 2), and a VCELL device is used as the y-axis detector 120 (FIG. 2). A VCELL device detects the radiation in only
20 one axis. Therefore, in order to detect an x-plane and y-plane direction, two nonparallel VCELLS are formed on the IC surface.

A VCELL of the present invention is illustrated in FIG. 3 and is designated generally throughout as reference numeral 126. FIG. 3 is a cross-sectional view of a
25 single VCELL device 126 that is formed as a conventional monolithic silicon IC. The VCELL includes two identical, yet opposing, phototransistors 128 and 130, formed in the silicon wafer. Generally, the phototransistors are formed in the silicon substrate 142 in the <100> plane 132. The <111> plane 134 is the silicon plane that is at an angle of 54.7 degrees from the <100> plane 132. The phototransistors 128 and 130 are formed in the
30 surface of the chip, primarily in the <100> plane, but with a base region extension down the <111> plane 140 such that the P type base regions 140 in the <111> plane 134 are

formed opposing and convergent with the $\langle 100 \rangle$ base regions 138. The structure formed is a v-groove 129 having a $\langle 100 \rangle$ plane horizontal structure 127 at the most convergent point (bottom) of the v-groove.

5 Each phototransistor 128 and 130 is a bipolar junction transistor having two rectifying PN junctions formed from extrinsic semiconductor materials of the P type and the N type. The phototransistors are NPN transistors. The transistors 128 and 130 are formed on an N type silicon substrate 142. The silicon substrate forms the collector of each phototransistor, 128 and 130. In addition, the phototransistors include a P type base
10 that includes a P type base region 138 in the $\langle 100 \rangle$ plane 132 and a P type base region 140 in the $\langle 111 \rangle$ plane 134. The emitters 136 are heavily doped N type and are formed in the $\langle 100 \rangle$ plane, 132.

 The phototransistors 128 and 130 that form the VCELL device 126 also include a
15 silicon dioxide (SiO_2) layer 146 and an interconnect layer 144 consistent with standard silicon planar process technology. The interconnect layer 144 is typically aluminum, or aluminum with a small amount of silicon (typically 1-2%), deposited as a thin film layer on the chip. The introduction of silicon in the aluminum interconnect layer 144 minimizes surface pitting by the aluminum during processing. A second important role
20 for the interconnect layer is that it is designed to minimize the generation of photocurrents in 128 and 130 in the $\langle 100 \rangle$ plane 132 when the surface of the chip is exposed to impinging radiation.

 The phototransistors 128 and 130 of the VCELL device 126 detect impinging
25 radiation. The impinging radiation is received, at an angle of incidence relative to the IC's surface or the $\langle 100 \rangle$ plane, on the $\langle 111 \rangle$ P type bases 140. The impinging radiation creates a photocurrent in the PN junction of the P type base 140 and the N type substrate 142. In essence, this PN junction behaves like a photodiode, and it can be modeled as such, providing a photocurrent into the $\langle 100 \rangle$ base 138 that is subsequently amplified by
30 the transistor.

The VCELL device as shown in FIG. 3 is modeled by the equivalent circuit in FIG. 4. The schematic equivalent of the single axis VCELL is designated generally throughout as reference numeral 148. A voltage source V_{CC} 150 provides voltage to the device and by design is the voltage applied to the IC substrate 142. This voltage source can be of a type known to those skilled in the art. The circuit diagram of the single axis VCELL detector includes emitters 164 and 166 corresponding to the N type heavily doped silicon emitters 136 (FIG. 3). The collector regions 160 and 162 correspond to the N type silicon substrate 142 (FIG. 3). In addition, the base terminals 168 and 170 of the VCELL 148 correspond to the P type silicon bases both in the $\langle 100 \rangle$ plane 132 (FIG. 3) and the $\langle 111 \rangle$ plane 134 (FIG. 3). The photocurrent sources 156 and 158 modeled in the circuit diagram represent the photocurrent generated by the absorption of the incident radiation by the PN junction formed between the P type silicon bases in the $\langle 111 \rangle$ planes 140 and the n-type substrate 142. Due to the circuit design, the transistors 152 and 154 behave as amplifiers, amplifying the photocurrents from the current sources 156 and 158. The PN junction between the P type silicon bases on the $\langle 111 \rangle$ planes and the N type silicon substrate are modeled in the circuit by diodes 149 and 151. The model current sources 156 and 158 are connected between the transistor bases 168 and 170 and the transistor collectors 160 and 162 shown in FIG. 4. Additional bias voltages can be applied to the transistors 152 and 154 at their base and emitter terminals 168, 164, 166 and 170, as required, by those skilled in the art.

FIG. 4 is a schematic drawing of a single axis VCELL. A single VCELL can only detect a single directional dimension of the impinging radiation. Two VCELL devices are required to detect a second directional dimension of the same impinging radiation. FIG. 5 models the dual VCELL device required to receive both a first and second directional dimension of impinging radiation on an IC surface. Dual axes detector 172 includes two VCELL devices 174 and 176. The VCELL devices must be arranged on the chip surface so that the devices sense different dimensions of the impinging radiation. Different dimensions can be defined by an x-axis directional dimension and a y-axis directional dimension. Physically, the VCELL detectors must be arranged nonparallel.

For example, if the VCELL detectors were arranged parallel, then the devices would receive radiation in the same directional dimension, thereby only detecting a single rectangular coordinate value in a single dimension. To completely determine the angle of elevation and azimuth of the incident radiation, two independent directional measurements are required at different angles to the incoming radiation. This allows calculation of the azimuth and elevation of radiation impinging the surface of the IC.

In general, it is not necessary that the two chosen directional dimensions, X and Y be orthogonal. In the present embodiment, in order to take process advantage of the relationship between the <100> axis and the <111> axis of single crystalline silicon, the X and the Y axes orientation are orthogonal in this embodiment.

The PN junction of the N type substrate 142 and the P type base 140 in the <111> plane is modeled in the circuit schematic photodiodes 178, 180, 182, and 184 (Fig. 5). The photocurrent I_P , produced in a PN junction is expressed as a function of the angle of incidence of the radiation, θ , by the following equation

$$I_P = A * \sin\theta$$

If scattering effects (and any other second order effects such as shadowing by surface objects at very small angles of incidence) are neglected, A is essentially independent of θ . Otherwise, the dependence of A on θ must be taken into account. This fact does not change the generalized analysis and results presented herein in any significant way for angles of incidence greater than typically 1 (one) degree. If phototransistors or photodiodes are fabricated on different planes in the silicon, then the above expression can be modified to give the value of photocurrents in these devices relative any reference. For example, if the reference plane is the <100> plane in silicon 132 (FIG 3), then the equation, including the offset, for the photocurrent produced along the x-axis, in an offset plane, is:

$$I_P = A * \sin(\theta_x \pm \text{offset})$$

The choice of \pm in the equation above depends on which opposing plane is chosen.

Assuming the configuration as shown in FIG. 2, the device has 3 detectors, an x-axis detector 118, y-axis detector 120, and a reference detector 122. The photocurrents produced in the x-axis detector are I_{px1} and I_{px2} . The resulting current behavior is illustrated in the graph shown in FIG. 6A. The reference transistor photocurrent is I_{ref} . The currents in the current sources I_{px1} and I_{px2} are indicated by graph lines 186 and 190. Under the assumption that scattering can be neglected to a first order and also under the assumption that the offset angle is 54.7 degrees (the $\langle 111 \rangle$ plane in silicon forms a 54.7 degree angle with the $\langle 100 \rangle$ plane), the graph in FIG. 6A defines the current behaviors in the detectors. The plots in the graph in FIG. 6A are shown normalized.

A reference transistor (or detector) 122 (FIG.2) produces a photocurrent, I_{ref} . The normalized output of the x-axis VCELL is thus given by the equation

$$I_{NX} = [I_{px1} \ I_{px2}] / I_{ref}$$

The above equation of normalized output I_{NX} is plotted in FIG. 6B.

20

An alternative normalization can be accomplished by normalizing using the sum of all currents for one axis. In this alternative case,

$$I'_{NX} = [I_{px1} \ I_{px2}] / [I_{px1} + I_{px2} + I_{ref}]$$

25

This alternative normalization form is useful when a normalized output that varies from +1 to -1 is required over a range of angle of incidence of 0 – 180 degrees. The curvature shown in Fig. 6B can thus be avoided as required.

30 The normalized output of the y-axis VCELL is:

$$I_{NY} = [I_{py1} - I_{py2}] / I_{ref}$$

The equation for the normalized VCELL output signal for the X-axis detector is:

$$I_{NX} = [I_{px1} - I_{px2}] / I_{ref} = [\sin (\theta_x - 54.7^\circ) - \sin (\theta_x + 54.7^\circ)] / \sin \theta_x$$

The equation for the normalized VCELL output signal for the y-axis detector is:

$$I_{NY} = [I_{py1} - I_{py2}] / I_{ref} = [\sin (\theta_y - 54.7^\circ) - \sin (\theta_y + 54.7^\circ)] / \sin \theta_y$$

The above equations are not accurate for angles of incidence less than 1 (one) degrees. In this case surface-shadowing effects must be taken into account.

All of the above-described photocurrents get multiplied by the gain factor ($\beta+1$) of the matched transistors that make up the VCELL detectors and the reference detector. The $\beta+1$ gain factor drops out with normalization. However, in all cases, the actual output of each detector is the emitter currents.

The currents produced by the X-axis detector 118 and the y-axis detector 120 of FIG. 2 provide the angle of incidence information of the incoming radiation for the two planes, θ_X and θ_Y . The computational device 504 124 calculates the azimuth θ_Z and the elevation ϕ of the incident radiation by applying the following formulas:

$$\tan \theta_Z = \tan \theta_X / \tan \theta_Y,$$

and

$$\tan \phi = \{ [1/\tan^2 \theta_X] + [1/\tan^2 \theta_Y] \}^{1/2}$$

The computational device 504 124 and the interface device 506 any additional signal processing electronics can be integrated along with 116 into a single device monolithic silicon IC chip. ~~Similarly, the interface device may not be used.~~ In addition,

the output of the computational device 504 124 can be either analog or digital as desired. All these options are known to those skilled in the art.

5 FIG. 7 shows a topographical view of the photolithographic mask pattern 192 used to fabricate the VCELL sensor 116. The reference phototransistor 198, an X-axis VCELL 194 and an orthogonal y-axis VCELL 196 and a typical input/output bond pad 200 are indicated.

10 FIG. 8 provides a more detailed drawing 202 of a VCELL device. Included in the figure are numerous photolithographic mask layers; a first mask layer 208, a second mask layer, a third mask layer 206 and 212, and a fourth mask layer 210 and 214.

15 FIGs. 9A-9D show different views of a general VCELL structure indicating the various masking patterns used. FIG. 9A shows the first mask shape 218 including the active base regions for the <100> transistors 222 and 224 and the region used to create the <111> base regions for the phototransistors 220. FIG. 9B shows the resultant creation of the <111> plane in the silicon through the use of the second mask layer. FIG. 9C depicts those areas where N⁺ silicon is formed as a result of using the third mask layer 206 and 212. The phototransistor emitter regions are indicated as 230. Area 228 is used
20 to separate the two VCELL phototransistor <111> base regions. FIG. 9D is a close-up view of contacts 416 to a phototransistor base region next to an emitter area 230.

25 FIGs. 10A-10I provide a series of drawings showing a set of typical process steps for fabricating a general VCELL sensor structure. In FIG. 10A, silicon substrate 380 suitable for monolithic silicon integrated circuit manufacture includes N type silicon with a planar surface, a <100> orientation, and a resistivity of typically 6 ohm-cm. The thickness of the silicon substrate is approximately 14 mils. A Silicon Dioxide (SiO₂) layer 400 is formed on the top surface of substrate 380 having a thickness of approximately 4,000 angstroms.

30

A layer of photoresist is applied as a continuous layer on the surface of the SiO₂ layer 400 376 and selectively irradiated using a photolithography system. A first mask is used to implement the selective irradiation, projecting the image as shown in FIG. 9A. The first mask delineates the areas that will form the first boron deposition. The photoresist is developed and the irradiated portions are removed to provide the opening 383 (FIG. 10B) in the remaining oxide 378 after a subsequent oxide etch process. All photoresist masking operations use standard photolithography techniques known to those skilled in the art for silicon planar processing technology.

In FIG. 10C, photoresist has been stripped, the oxide aperture has been etched and ~~doped-P- base region 386 is implanted or~~ and diffused into substrate 380 by subjecting the structure to ion implantation of boron ~~or~~ and by thermal diffusion by subjecting the wafer to high temperature ~~with a source of boron dopant such as boron nitride wafers.~~ The boron deposition and subsequent diffusion/oxidation forms a P-region 386 with a junction depth of .8-1 micron and a sheet resistance of approximately 300ohm/sq. Oxide layer 388 is grown on the substrate 380. The oxide layer has a thickness of approximately 2,000 angstroms over the P-region 386.

A layer of photoresist is applied to the silicon substrate 380. A second mask is used to implement the selective ~~irradiation silicon <111> etch,~~ resulting in projecting the image as shown in FIG. 9B. The second mask delineates the areas which will receive a first silicon etch, a second boron deposition and a second silicon etch. The base 220 remains as previously developed, and the rectangular image 226 is projected onto the surface of the wafer. Thereafter, the photoresist is developed and the irradiated rectangular portion 226 is ready for subsequent processing.

In FIG. 10D the v-groove 390 is preferentially etched (the first silicon etch) forming the opposing convergent sidewalls 394 and 392 oriented in the <111> plane. Etching is performed where the <100> plane is etched approximately thirty (30) times faster than the <111> plane using a wet chemical preferential etching solution of KOH, IPA and H₂O at 80 C°. The <111> plane in silicon intersects the <100> plane at an angle

of 54.7 degrees. Therefore, the resulting structure is shown with a v-groove having an angular slope from the <100> plane of 54.7 degrees. ~~In addition,~~ The the first silicon etching separates the boron doped (P type) <100> region 386 (FIG. 10C) into two separate and distinct P-type base regions in the <100> plane, 396 and 398.

5

In FIG. 10E a second doped P type region 400 is implanted into substrate 380 by subjecting the structure to ion implantation of boron or by thermal deposition and diffusion/oxidation with a boron dopant source such as boron nitride wafers. The second Boron deposition forms a P type region in the <111> planes 394 and 392 as well. The
10 second P type regions 394 and 392 have a junction depth of ~~approximately 0.8~~ less than 1.0 microns.

In FIG. 10F, a second silicon etch is performed on the v-groove 390 providing additional depth of ~~approximately less than 1-2~~ 1-2 μ (microns). This further etching allows
15 for the separation of the boron-doped P-region 400 leaving only a P type base region 402 on the <111> plane and a P type base region 404 on the opposing <111> plane. The opposing P type base regions on the opposing <111> planes form part of the base regions of the NPN phototransistors.

20 In FIG. 10G, an oxide layer 403 is grown on the bare silicon regions in the v-groove 390. The oxide layer has a thickness of approximately 2,000 angstroms. This oxidation masks the silicon surfaces such that when masking the surface to apply the N^+ depositions the doping will not penetrate areas other than those to be doped.

25 A layer of photoresist is applied across the entire wafer. A third mask is used when implementing the selective irradiation, creating the image as shown in FIG. 9C. This masking step delineates the regions where the N^+ doped areas 230 and 228 (FIG. 9C) are formed. The N^+ regions are formed using either ion implantation or thermal diffusion using a source of phosphorous or arsenic or both. The N^+ regions 230 form the
30 emitters for the bipolar phototransistor. The N^+ regions 228 provide a means of separation between the boron doped P type <111> planes formed in FIG. 9B by the end

sections of 226. This provides that the phototransistor devices are conductively isolated from each other. The base 220 remains as previously formed.

5 With reference to FIG. 10G, the photoresist is developed and the irradiated portions are removed providing the openings 406 and 407 for emitters after an oxide etch process.

10 The heavily doped N^+ regions 408 and 410 are formed in substrate 380 by subjecting the structure to ion implantation or thermal diffusion of phosphorous or arsenic. In addition, with reference to FIG. 9C, the end regions of the v-groove 228 are heavily doped in order to terminate the p type $\langle 111 \rangle$ base regions (converting the P regions in this area back to N regions). The phosphorous depositions form N^+ regions, 408 and 410, that serve as the emitters of the phototransistors. The N^+ regions have a junction depth of approximately 1.0-1.5 microns.

15

With reference to FIG. 10I, a layer of photoresist is applied on the silicon and a fourth mask is used to create the contact openings 416 to the P type base regions and 418 to all N^+ type material emitter regions. The photoresist is selectively irradiated using the photolithography system and the fourth mask, then the irradiated portions are removed to provide a consecutive line of openings to serve as the P type base contacts 416 and provide all contacts to the N type material, including the N^+ emitters.

20

FIG. 9D illustrates the placement of the P type base contacts 416 along the substrate surface. The consecutive arrangement minimizes the effect of base spreading resistance by reducing the series resistance inherent in the silicon material used in the P type base regions, 402, 404, 396 and 398. (FIG. 10F).

25

Further processing steps in the fabrication of ICs are known in the art and further include forming an interconnect metallization layer forming contacts to the the P type base regions 416 (FIG. 10I) and the N^+ emitters 408 and 410 (FIG. 10H), then masking

30

the interconnect metallization pattern to form the interconnects to the bond pads on the chip ~~from the contacts~~.

Generally, the exemplary embodiment described herein includes ~~an~~ a monolithic
5 silicon integrated circuit device having three phototransistors including two <100>
phototransistors having bipolar junction transistors and a reference phototransistor. One
of ordinary skill in the art will recognize that the v-groove structure disclosed that makes
up the opposing and convergent P type base regions of the phototransistors can be made
using various planes, surfaces and geometric configurations. The present invention is not
10 limited to P-type base regions formed in a <111> plane. In addition, one of ordinary skill
in the art will recognize that the choice of bipolar junction phototransistors is also not
limiting. Other devices, PNP (as opposed to NPN as described) transistors, MOSFETS,
or other types of devices can be employed to serve the function of the NPN
phototransistors amplifiers in the preferred embodiment.

15 Also, various methods of processing are available in the art to form other various
planes, surfaces or geometric configurations. For example, methods including ion
milling, plasma etching, micro-electro-mechanical structuring (MEMS), or micro-
machining are available to form various other planes, surfaces and geometric
20 configurations. The present invention is not limited to the crystallographic method
described herein. The embodiment disclosed herein is an exemplary embodiment of the
present invention.

In addition, the present invention includes other numerous variations available to
25 the embodiment described herein. For instance, the IC can include a single VCELL
device or numerous VCELL devices on the surface of the chip depending upon the
application required of the IC. In addition, when required, the VCELL structure can be
halved such that it is formed using on a single transistor structure thus eliminating the
differential transistor structure. The system of the present invention can employ various
30 kinds of devices to perform the calculations required for determining azimuth and
elevation, including a microprocessor or a ROM device.

Those skilled in the art will readily implement the steps necessary to provide the structures and methods disclosed herein, and will understand that the device, system and method parameters, materials, and dimensions are given by way of an exemplary
5 embodiment of the present invention. These various parameters, materials, and dimensions can be varied to achieve the desired structure as well as any modifications of the present invention.

MARKED-UP COPY

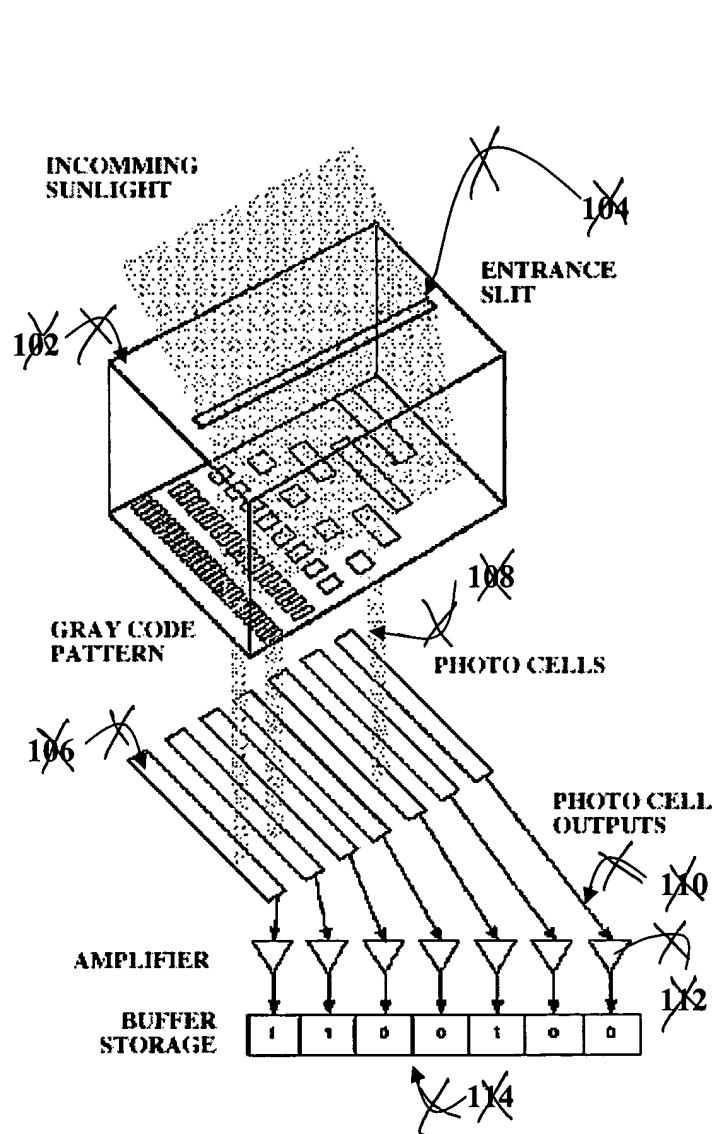
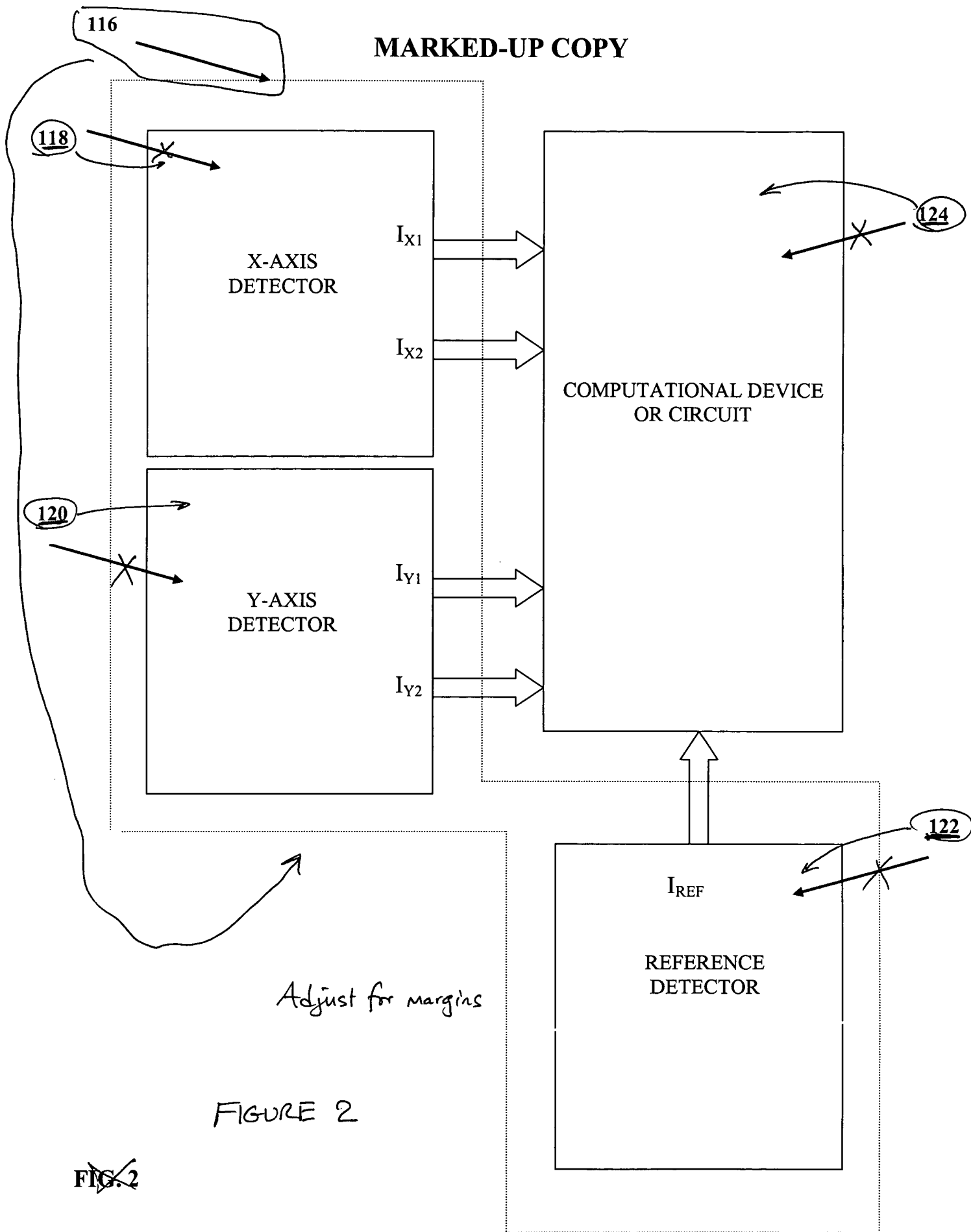


FIGURE
FIG. 1
(PRIOR ART)

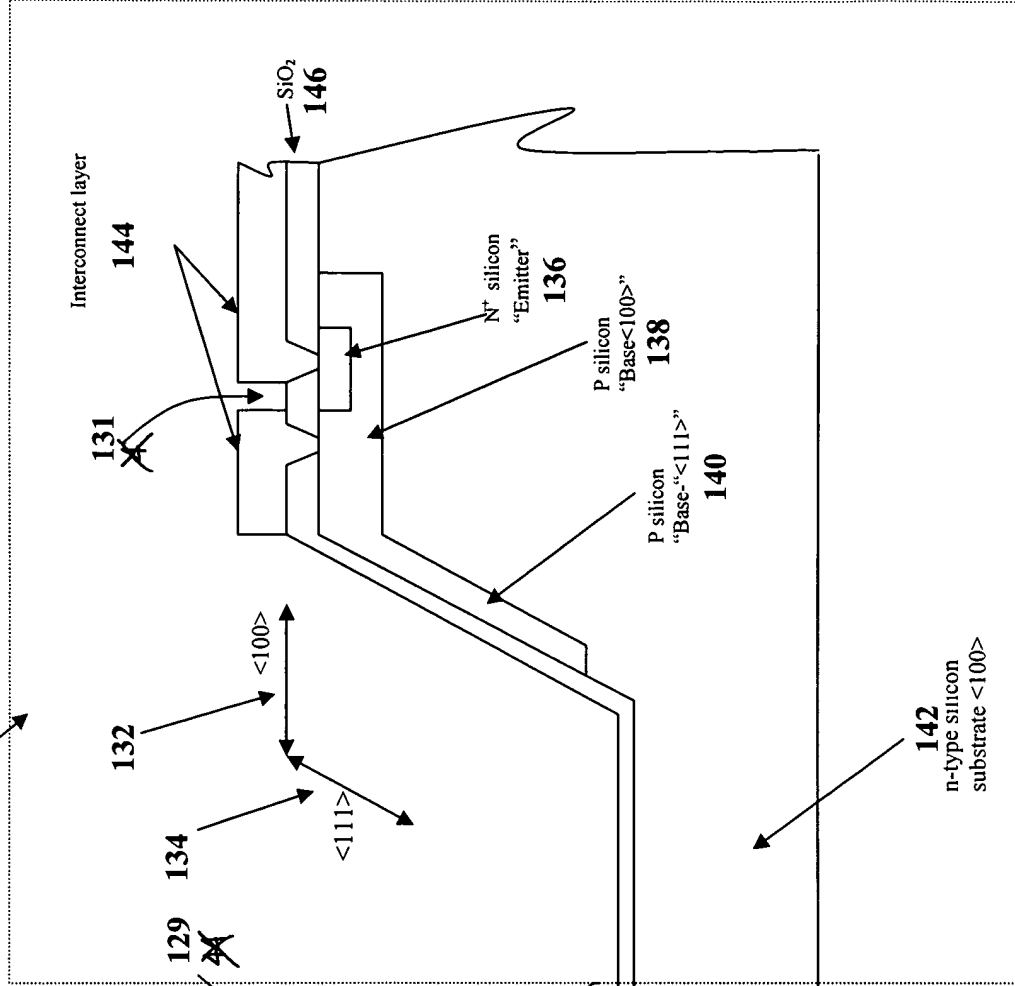
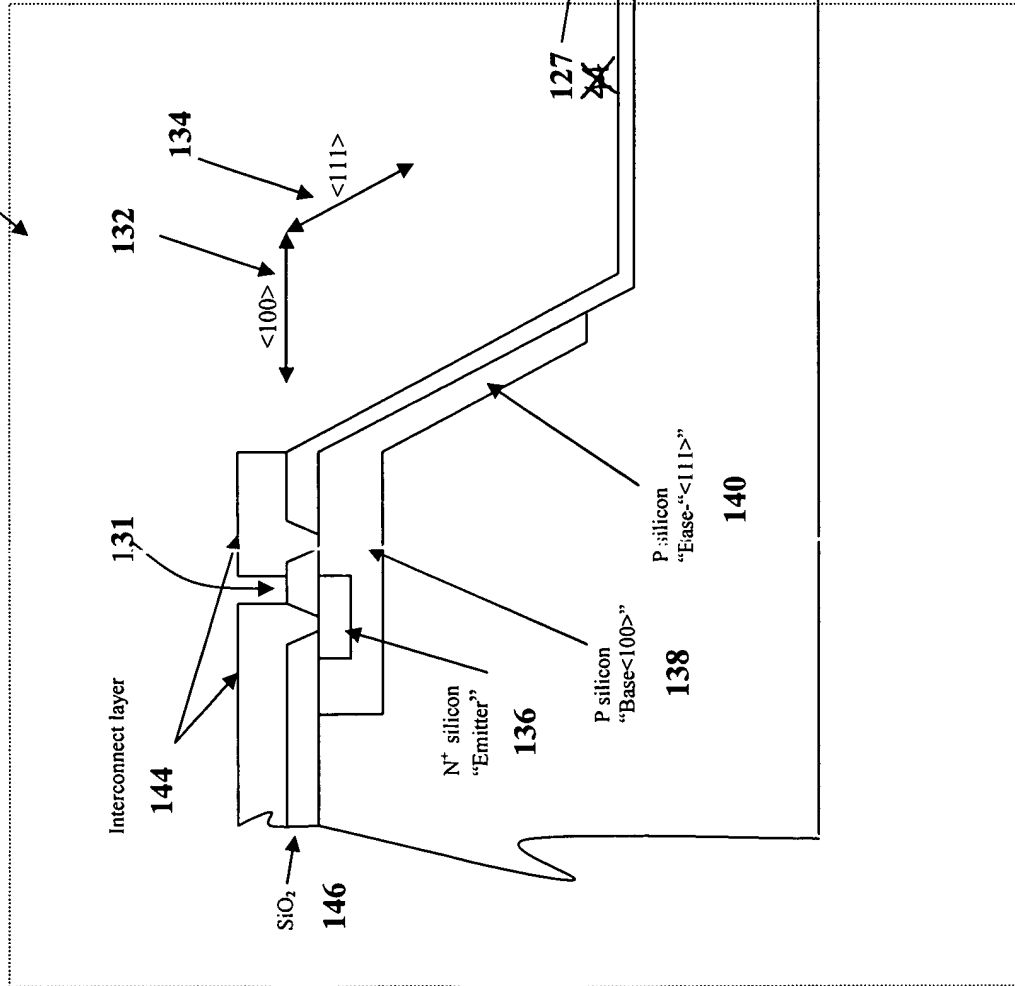
MARKED-UP COPY



126

MARKED-UP COPY
128

130



~~FIG. 3~~
FIGURE 3

Adjusted for margins

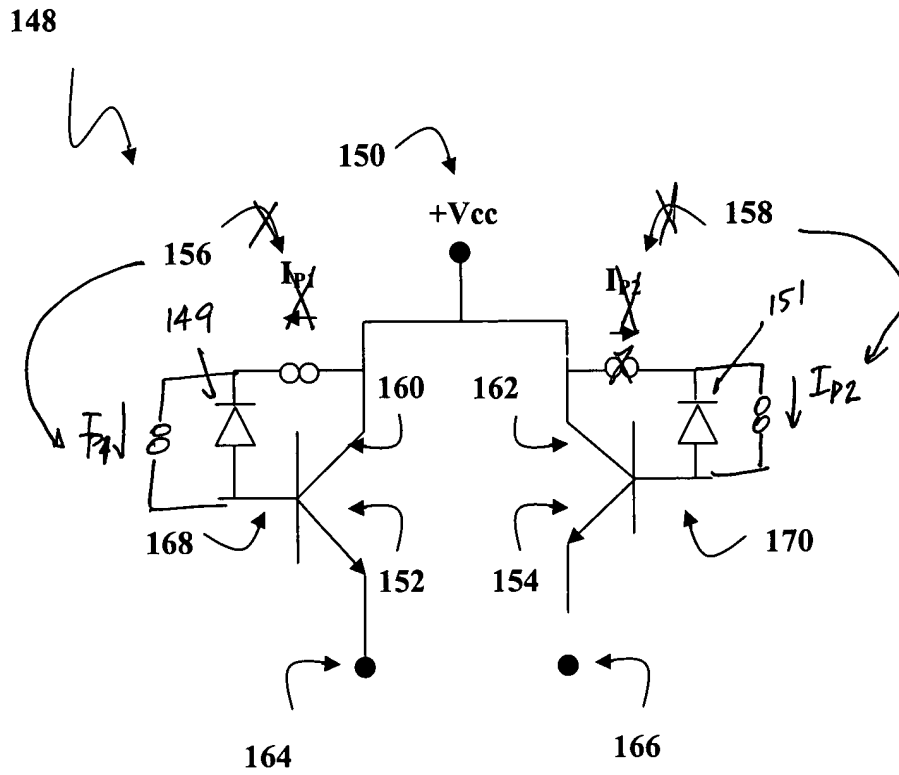
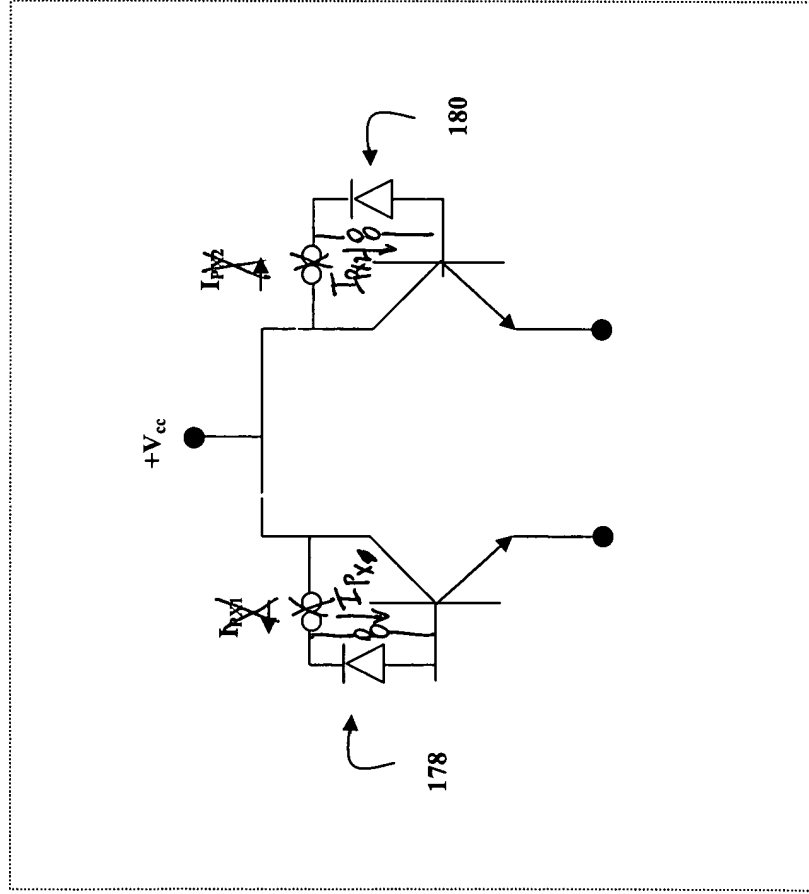


FIG. 4

FIGURE 4

172

174



176

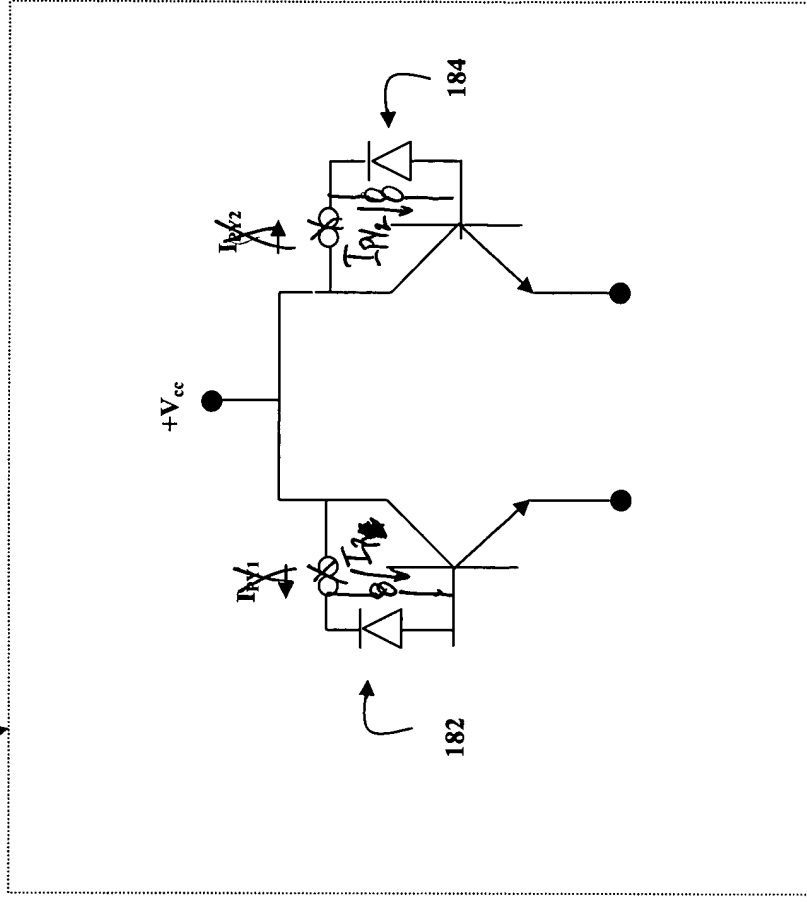


FIG. 5
FIGURE 5

Adjust for Margins

MARKED-UP COPY

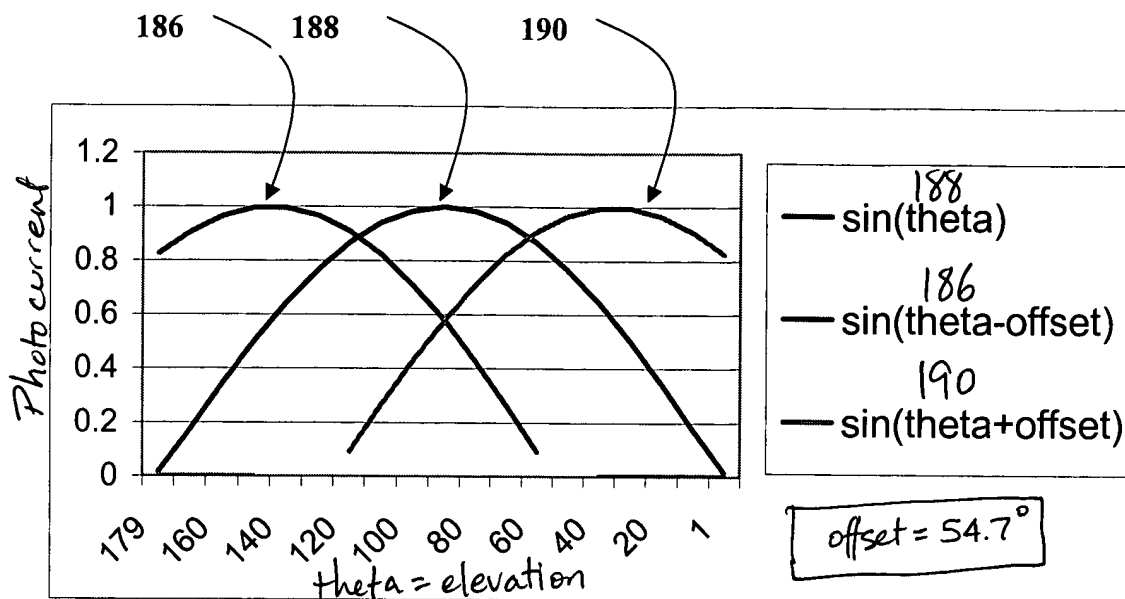
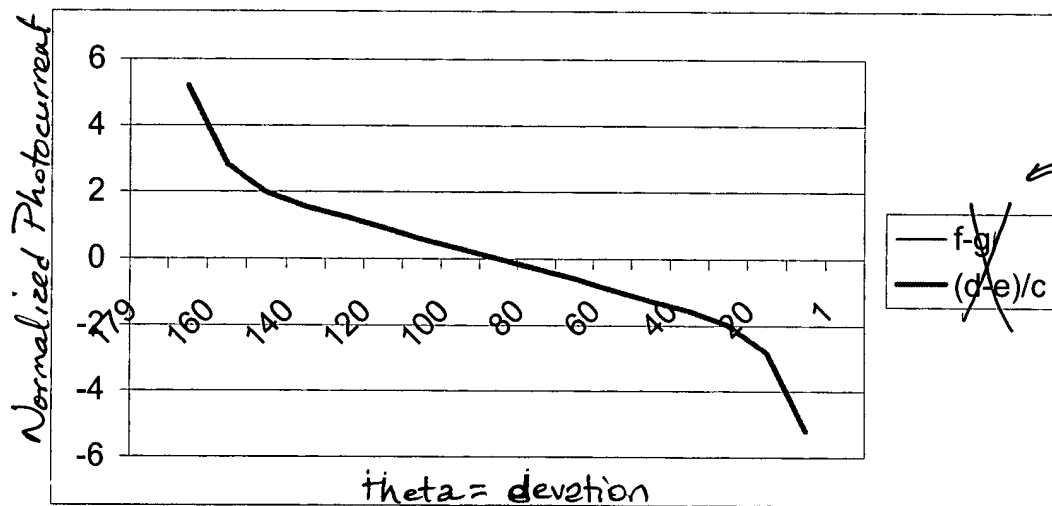


FIGURE 6A

~~FIG. 6A~~



~~FIG. 6B~~

FIGURE 6B

MARKED-UP COPY

192



198

194

200

196

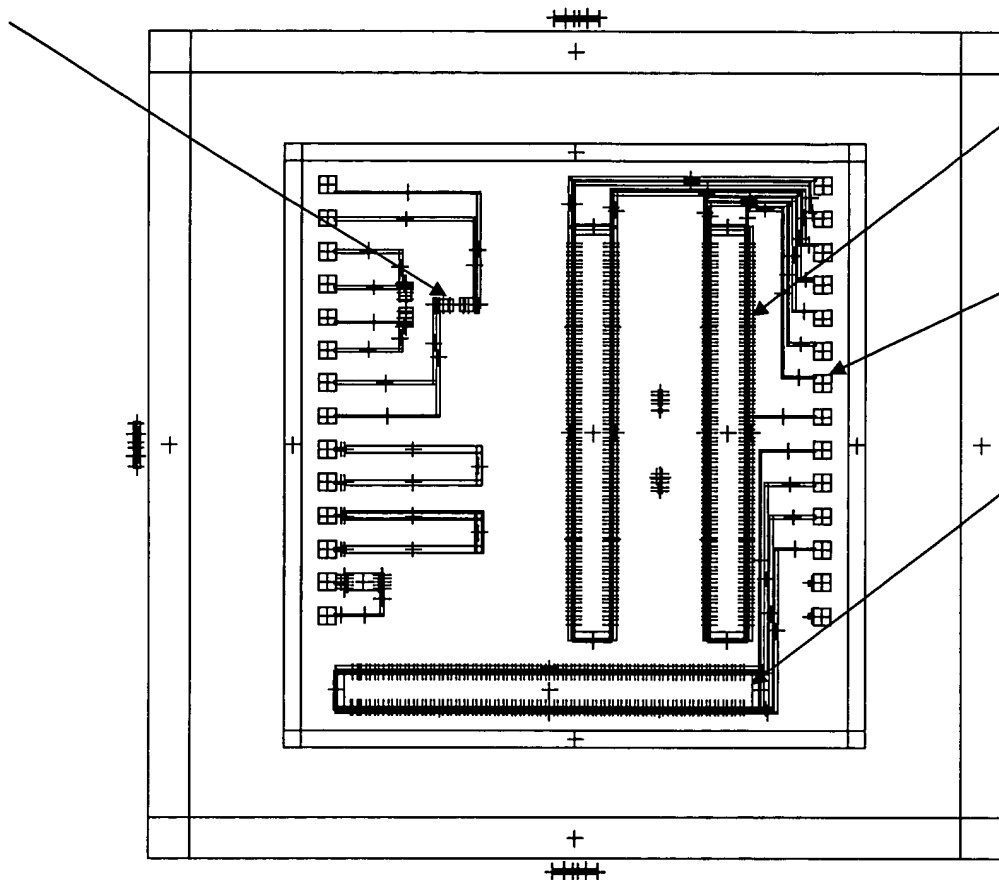
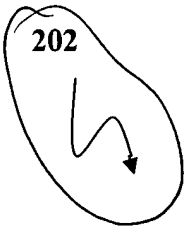
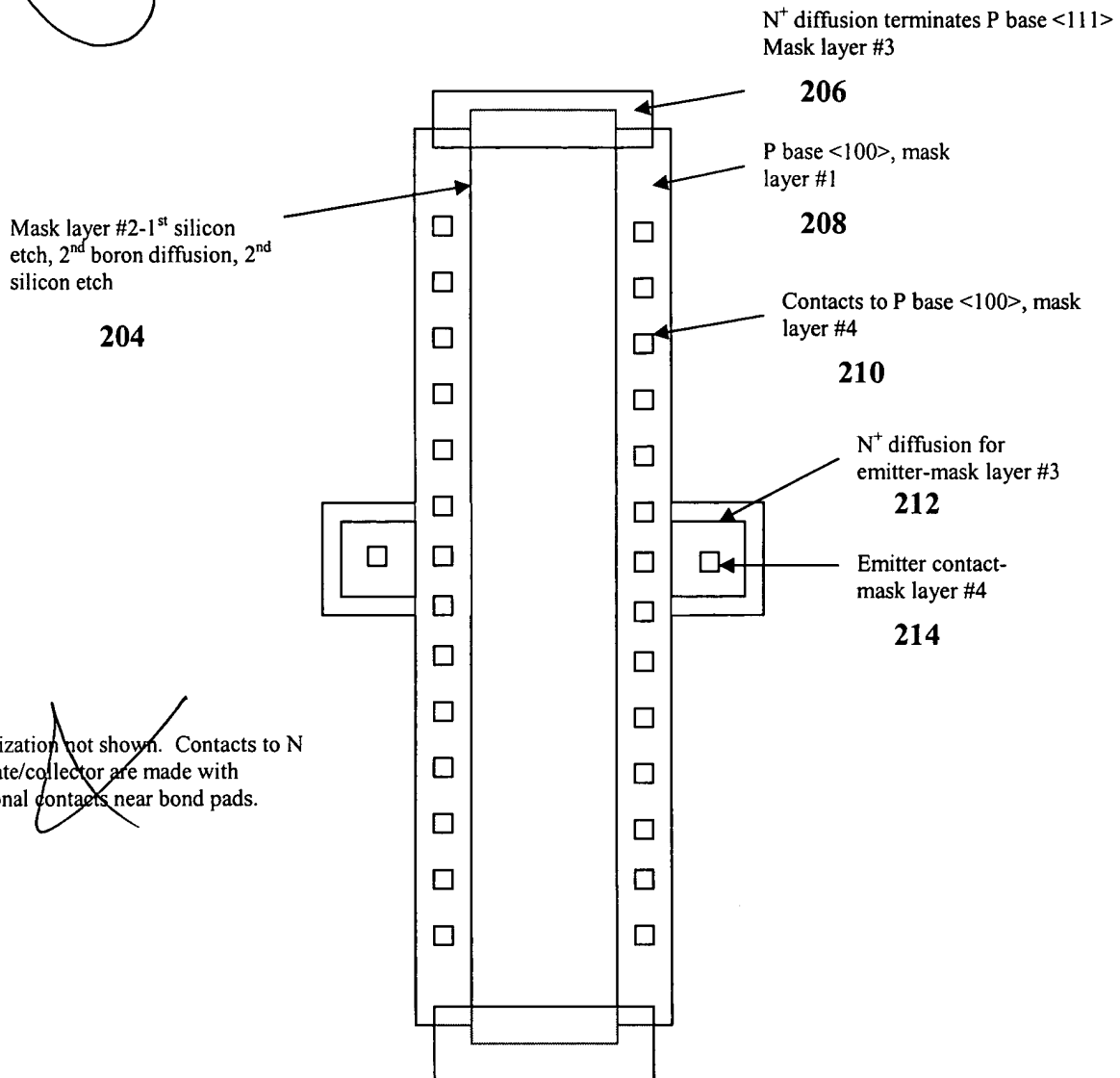


FIGURE 7
FIG. 7

Adjusted for
Margins



MARKED-UP COPY



~~FIG. 8~~
FIGURE 8

Adjusted for
Margins

MAR 14 2004

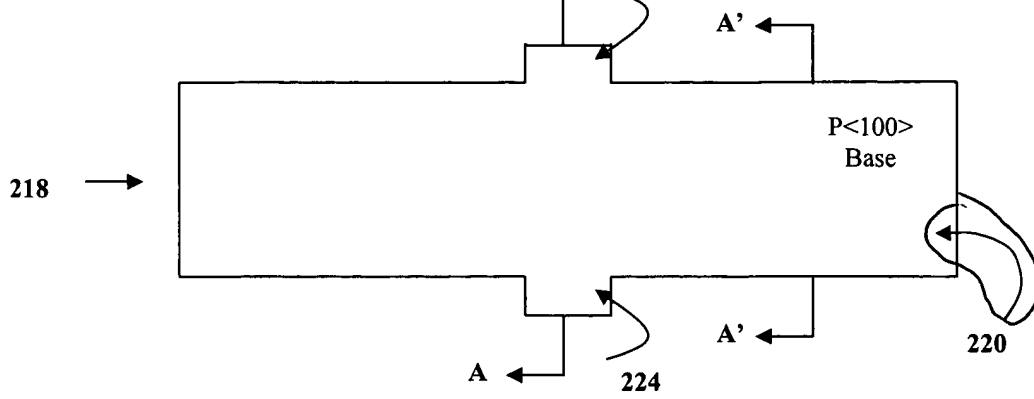


FIGURE 9A

~~FIG. 9A~~

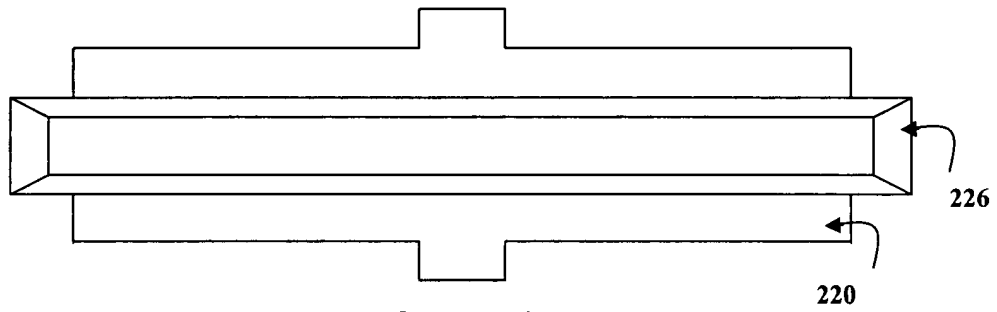


FIGURE 9B

~~FIG. 9B~~

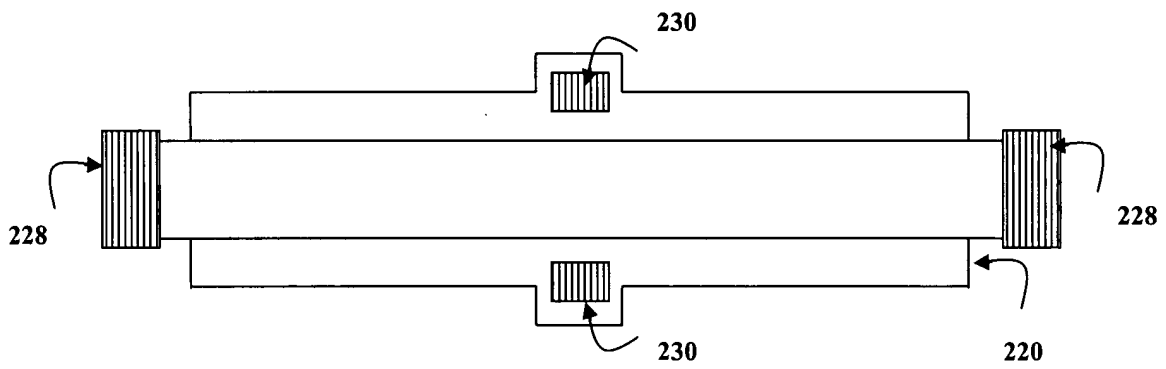
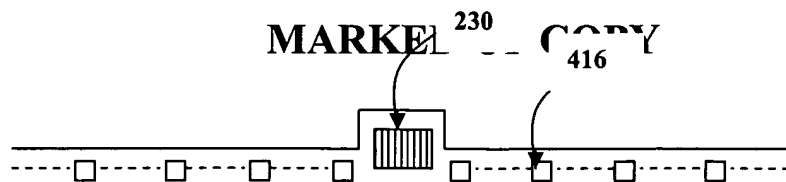


FIGURE 9C

~~FIG. 9C~~

Adjusted for
Margins



~~FIG. 9D~~
FIGURE 9D

Adjusted for
Margins

MARKED-UP COPY

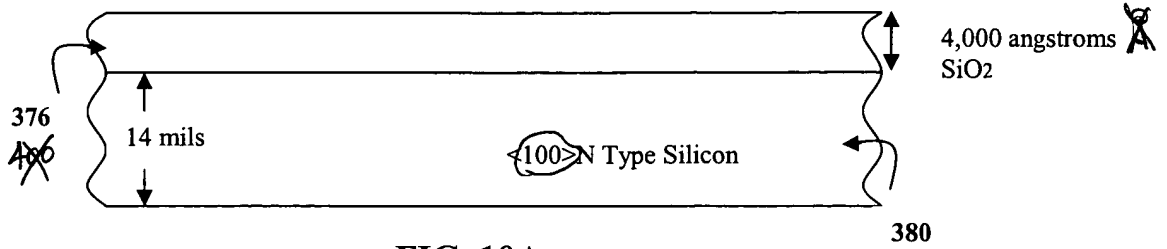


FIG. 10A
FIGURE

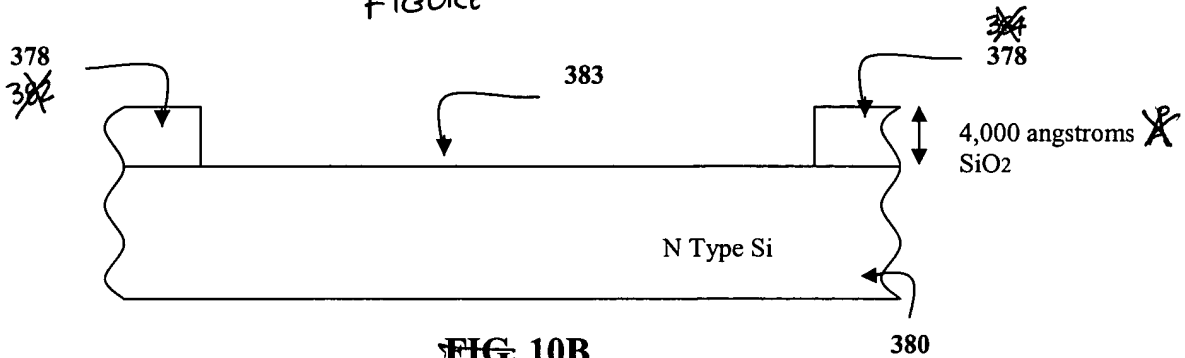


FIG. 10B
FIGURE

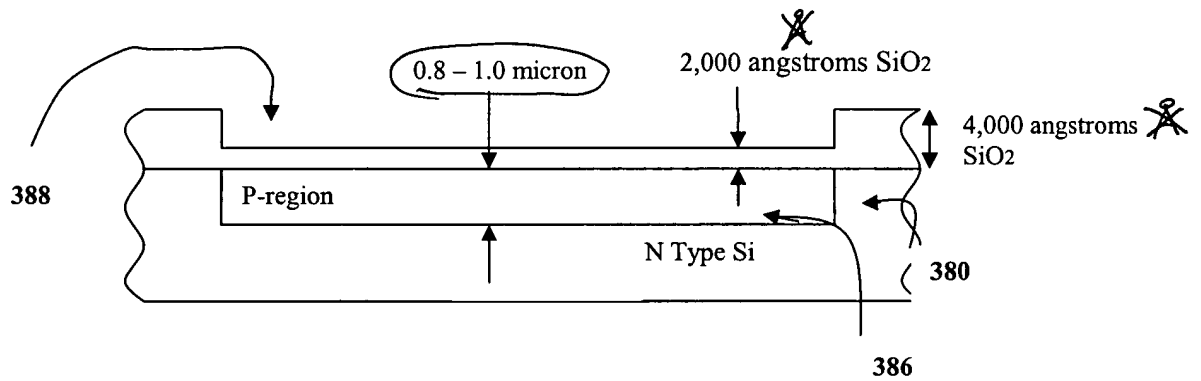


FIG. 10C
FIGURE

Adjusted for Margins

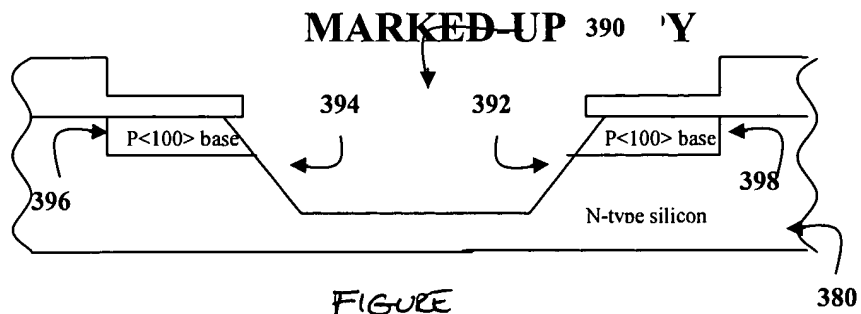


FIGURE
FIG. 10D

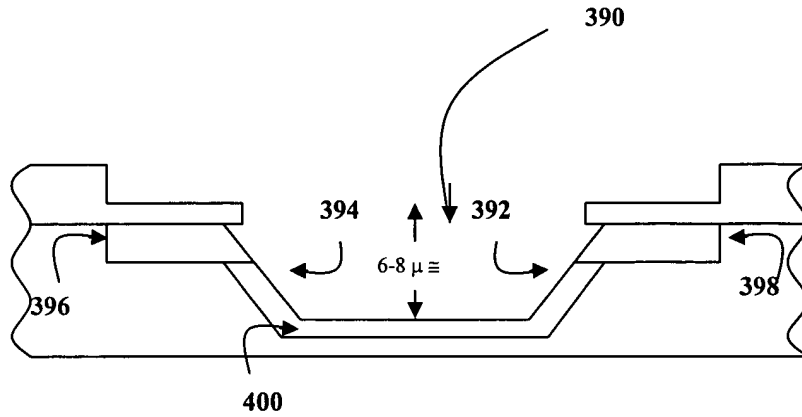


FIGURE
FIG. 10E

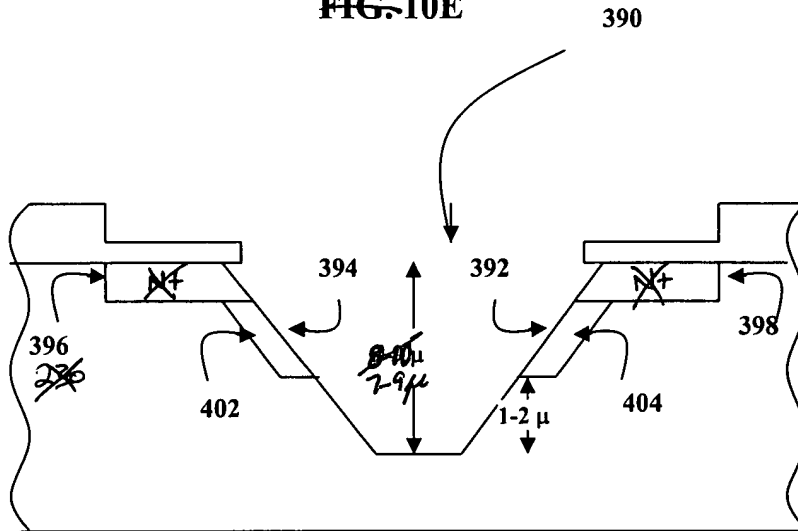


FIG. 10F
FIGURE

Adjusted for Margins

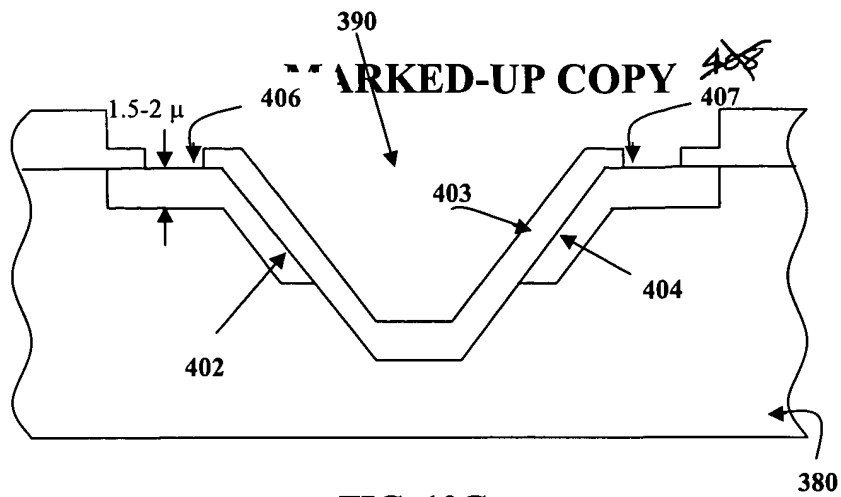


FIG. 10G
FIGURE

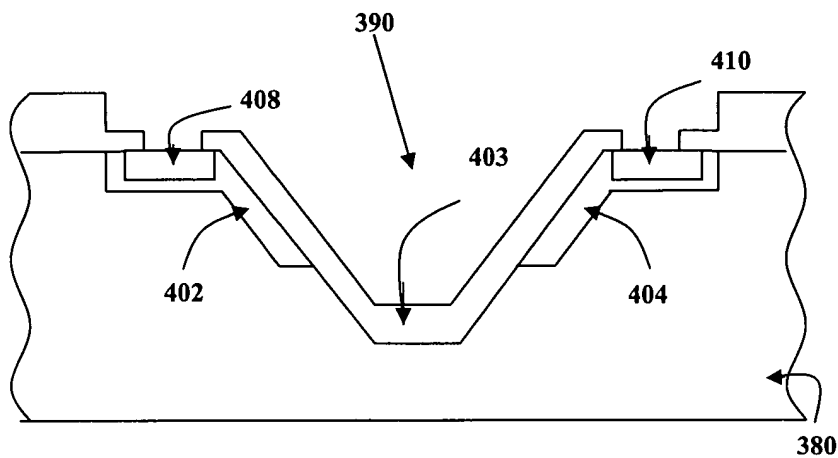


FIGURE
FIG. 10H

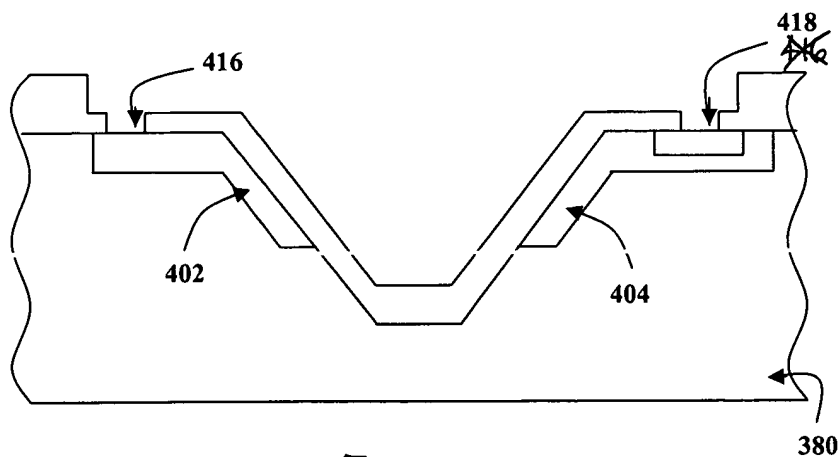


FIGURE
FIG. 10I

Adjusted for
Margins